Science of the Total Environment 648 (2019) 508–517

Contents lists available at ScienceDirect

Science of the Total Environment

journal homepage: www.elsevier.com/locate/scitotenv

Organic matter decomposition sustains sedimentary nitrogen loss in the Pearl River Estuary, China

Ehui Tan [a], Wenbin Zou [a], Xinlei Jiang [a], Xianhui Wan [a], Ting-Chang Hsu [b], Zhenzhen Zheng [a], Ling Chen [a], Min Xu [a], Minhan Dai [a], Shuh-ji Kao [a,*]

[a] State Key Laboratory of Marine Environmental Science, Xiamen University, China
[b] Earth System Science Program, Taiwan International Graduate Program, Academia Sinica, Taipei, Taiwan

HIGHLIGHTS

- Sedimentary nitrogen removal was predominated by denitrification relative to a minimal contribution from anammox.
- Sedimentary nitrogen removal involved mainly particulate organic form deposited onto sediments.
- The sediments acted as an important N_2O source, equivalent to ~35% of the daily N_2O emission in the Pearl River Estuary.

GRAPHICAL ABSTRACT

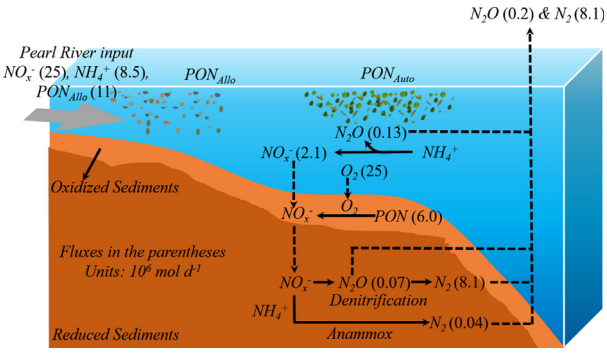

ARTICLE INFO

Article history:
Received 21 May 2018
Received in revised form 30 July 2018
Accepted 8 August 2018
Available online 08 August 2018

Editor: Ouyang Wei

Keywords:
Coupled nitrification-denitrification
Denitrification
Anammox
Isotope pairing technique
Nitrous oxide

ABSTRACT

The Pearl River Estuary (PRE) has long received tremendous amounts of anthropogenic nitrogen, and is facing severe environmental problems. Denitrification and anaerobic ammonium oxidation (anammox) are known to be two major nitrogen removal pathways in estuarine sediments. Through the use of slurry and intact sediment core incubations, we examined the nitrogen removal pathways and quantified the *in situ* denitrification and anammox with associated gaseous nitrogen production rates. Sedimentary nitrogen removal was predominated by denitrification (93–100%) relative to a minimal contribution (<7%) from anammox. Among the detected environmental factors, salinity, bottom water NO_x^- (nitrate and nitrite) concentration, sedimentary organic matter and dissolved oxygen consumption rates showed good correlations with denitrification and anammox rates. Sedimentary nitrogen loss was mainly supported by endogenic coupled nitrification-denitrification ($6.0 \pm 1.5 \times 10^6$ mol N d^{-1}), with water-column-delivered NO_x^- ($2.1 \pm 0.6 \times 10^6$ mol N d^{-1}) as the secondary source. Such results suggested that sedimentary nitrogen removal involved mainly particulate organic form (allochthonous or autochthonous) deposited onto sediments, rather than inorganic forms in overlying water. Meanwhile, total N_2O production from sediments was estimated to be $7.3 \pm 2.1 \times 10^4$ mol N d^{-1}, equivalent to ~35% of the daily N_2O emissions in the PRE.

1. Introduction

Excess anthropogenic nitrogen emission is becoming the second most serious global environmental issue and can potentially lead to

* Corresponding author.
E-mail address: sjkao@xmu.edu.cn (S. Kao).

https://doi.org/10.1016/j.scitotenv.2018.08.109
0048-9697/

irreversible ecological problems (Rockstrom, 2009). A tremendous amount of anthropogenic fixed nitrogen generated on continents is discharged into estuaries as excess nitrogen and ultimately delivered into the coastal oceans (Schlesinger, 2009). Estuaries, standing at the frontal zone of the ocean to the excess nitrogen input from land, serve as a natural bioreactor that transforms and removes reactive nitrogen, which is one of the key driving forces for coastal ecosystem development and degradation (Seitzinger et al., 2010). As a consequence of anthropogenic impacts, growing numbers and coverage of hypoxia and harmful algal blooms occur in the coastal oceans (Deegan et al., 2012; Qian et al., 2018). Thus, an improved understanding of the fate of excess nitrogen during transport in estuaries may facilitate for mitigation and control of nitrogen pollution and harmful algal blooms in coastal seas.

Nitrogen removal processes are critical in aquatic systems for maintaining homeostasis (Pennino et al., 2016). Microbially mediated denitrification and anaerobic ammonium oxidation (anammox) are the two most important nitrogen removal pathways (Mulder et al., 1995; Seitzinger, 1988). In a marine system, denitrification in continental shelf sediments was estimated to account for approximately 44% of total global denitrification (Seitzinger et al., 2006). For the estuarine ecosystems, Nixon et al. (1996) analyzed the annual total nitrogen budget for various estuaries around the North Atlantic and revealed that nitrogen removal can reach 30–65% of total input *via* sedimentary denitrification. However, recent research showed that in addition to denitrification, the presence of anammox could be crucial, although the relative importance of anammox to total sedimentary nitrogen removal varied significantly (Devol, 2015). For example, in the North Atlantic and the Cascadia Basin, anammox was found to contribute ~35–68% (Trimmer and Nicholls, 2009) and 12–51% (Engström et al., 2009) of sedimentary nitrogen removal, respectively. In contrast, the contribution of anammox was considered less important in estuarine sediments. For example, anammox contributed <1 to 11% in the estuaries of southeast England (Nicholls and Trimmer, 2009), whereas in many other estuaries, such as the Goa Estuary in India and Southwest Pacific island estuaries, anammox was found to be unimportant (Dong et al., 2011; Fernandes et al., 2012). Recent studies pointed out that organic matter and inorganic nitrogen concentration might be two important factors regulating anammox (Brin et al., 2014; Teixeira et al., 2016; Teixeira et al., 2012); however, factors controlling the relative importance of denitrification and anammox processes are still not well understood.

The Pearl River Estuary (PRE) is located in one of the most densely populated and industrialized areas of China. The PRE shares similar environmental problems with other major estuaries, such as eutrophication and hypoxia (Dai et al., 2006; Huang et al., 2003). The nitrogen pollution in the PRE has also become one of the most serious environmental issues. Previous studies focused mainly on the distribution of nutrients and their biogeochemical impacts on water bodies within the PRE (Huang et al., 2003; Qian et al., 2018) with less efforts paid to the sedimentary nitrogen removal processes.

Nitrous oxide (N_2O) is oversaturated (163–905% saturation) throughout the entire PRE, with high spatial variation (Lin et al., 2016). However, the sources of N_2O, which is derived from water column nitrification or sedimentary denitrification are not well elucidated in the PRE.

To provide a novel insight into the nitrogen fate in PRE sediments, including the pathways and mechanisms of nitrogen removal and associated N_2O emission, we applied the ^{15}N isotope pairing technique onto sediments in the highly nitrogen polluted PRE (1) to identify and quantify major nitrogen removal pathways, (2) to quantify the sedimentary N_2O production rate, and (3) to evaluate the effective environmental factors for nitrogen removal, thus to articulate the role of sediments in the estuarine nitrogen cycle and in climate under the context of anthropogenic influence.

2. Materials and methods

2.1. Study area

The Pearl River is the second largest river in China and the thirteenth largest in the world, in terms of discharge. The water discharge shows significant seasonal variation with an average discharge of 330×10^9 m^3 y^{-1}, and ~80% of the discharge takes place in the wet season from April to September (Dai et al., 2006). The river discharges into the South China Sea through three estuaries, namely, Lingdingyang Bay, Maodaomen Bay and Huangmaohai Bay. The focus of this study was on the Lingdingyang Bay, which occupies the largest part of the estuary and is traditionally referred to as the PRE. The width of the horn-shaped PRE ranges from ~5 km in the north estuary to ~50 km in the south estuary (Fig. 1). Most of the PRE is shallow, with a depth range from 2 to 5 m in the upstream and going deeper to ~20 m around the seaside entrance. The mean annual temperature across the PRE catchment ranges from 14 to 22 °C and the mean annual precipitation ranges from 1200 to 2200 mm (Zhang et al., 2008). The tidal cycle is dominated by a semi-diurnal mixed tidal regime with a mean tidal range of 1.0–1.7 m (Mao et al., 2004). A perennial salt wedge exists in the PRE, due to the seaward freshwater discharge and tidal cycle. The Pearl River delivers approximately 80×10^6 tons of sediments annually, and ~50% of the sediment is trapped inside the estuary (Liu et al., 2009). Consequently, sediment types in the PRE vary depending upon the hydrodynamics of the sedimentation environment. Overall, the PRE is an area of fine-grained sediments (~10 μm) and exhibits muddy patches with relatively coarse sediments (60–100 μm) in the north (Zhang et al., 2013).

2.2. Sampling and pretreatment

In this study, sediments and near-bottom water were collected during a cruise onboard R/V "Tianlong" to the PRE, from 16 through 27 November 2013, representing the dry season. Six sites along the salinity

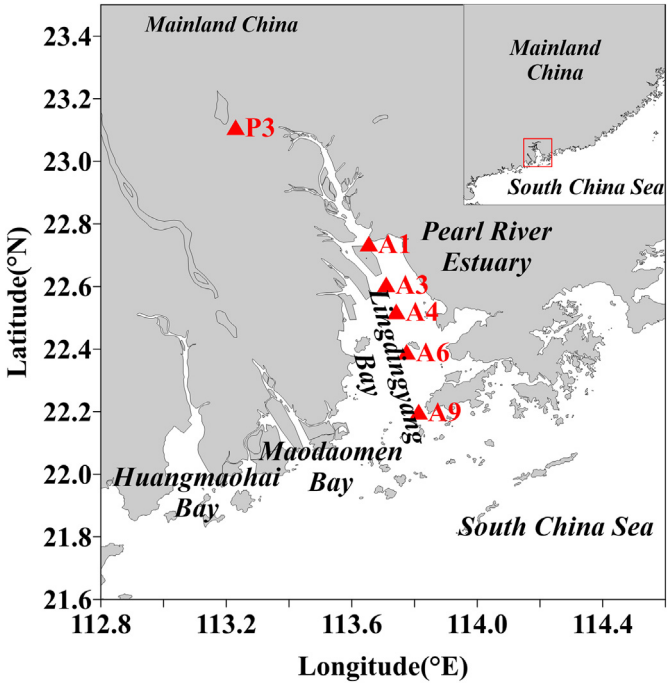

Fig. 1. Map of the Pearl River Estuary. Red triangles indicate sampling sites. (For interpretation of the references to colour in this figure legend, the reader is referred to the web version of this article.)

gradient in the PRE were sampled (Fig. 1). The bottom water for incubations and nutrient analyses was collected by using 12 L Niskin bottles attached to a conductivity-temperature-depth rosette sampler. Sediments were taken using a standard box corer (20 × 20 cm). The overlying water in the box corer was removed carefully to ensure that the sediment-water interface was not disturbed. Fifteen intact cores were then sub-sampled by inserting PVC tubes (inner diameter of 5 cm and length of 30 cm) into the bulk sediments. Subsequently, the near-bottom water in the same station was added to these intact cores to adjust to a height of 7 cm above the sediment surface. Among the 15 intact sub-cores, fourteen were incubated and the remaining one was probed for a dissolved oxygen profile in porewater. After the intact core sampling, the surface sediments (1 cm) were collected carefully in the residual box corer for slurry incubation and sediment characteristics analysis. All incubations were conducted immediately onboard. The surface sediments and bottom water samples were stored at −20 °C for physical and chemical characteristic analyses.

2.3. Determination of the dissolved oxygen microprofile and sedimentary consumption rates

Dissolved oxygen (DO) in the overlying water and porewater were measured for the intact cores by using an automated motorized micromanipulator, fitted with an oxygen sensor (OX 50, Unisense AS) and controlled by micro-profiling software (SensorTrace PRO, Unisense AS). A two-point calibration of the DO microsensor in water with a DO saturation of 0 and 100% was performed prior to usage. Measurements were done with high spatial resolution intervals of 0.2 mm. The DO profiles were measured initially at 0.3 cm above the sediment-water interface and ended at the depth with no oxygen. The oxygen penetration depth (OPD) is a measurement of infiltration of oxygen from the overlying water to the surface sediments, representing the thickness of the aerobic sediment layer. Based on the DO profile, the OPD was determined from the sediment-water interface, to the depth where no oxygen was detected.

Two methods were applied to calculate the sedimentary DO consumption rate. Firstly, we applied a conventional method (hereafter referred to as the diffusion method) supported by Fick's first law under steady state conditions (Schulz, 1999),

$$J = \phi \times D_{sed} \times {}^{\partial C}\Big/_{\partial z}, \tag{1}$$

$$D_{sed} = {}^{D^{sw}}\Big/_{\theta^2}, \tag{2}$$

$$\theta^2 = 1 - \ln\left(\phi^2\right), \tag{3}$$

where J represents the DO consumption rate. ϕ is the sediment porosity. D_{sed} and D^{sw} represent the molecular diffusion coefficient for oxygen in sediments and seawater, respectively. Here, D^{sw} is fixed to be 1.91×10^{-9} m^2 s^{-1} at 20 °C in seawater. θ is the calculated sediment tortuosity. $\partial C/\partial z$ is the DO concentration gradient under steady state conditions. $\partial C/\partial z$ is derived from the DO profile, where it exhibits the highest inclination below the sediment surface (Schulz, 1999).

For cross-checking comparison, we calculated the DO consumption rate by using the difference of DO concentration in the overlying water before ($[DO]_{before}$) and after ($[DO]_{after}$) the sediment intact core incubation (hereafter referred to as the incubation method).

$$J = h \times \frac{[DO]_{before} - [DO]_{after}}{T}, \tag{4}$$

where h is the height of water column in the sediment intact core and T is the incubation time.

Since irrigation was reported to be the predominant process in controlling solute transfer across the sediment-water interface in the PRE (Cai et al., 2015), we thought that the diffusion method underestimated the DO consumption rate, because it does not consider the influences of physical and/or bio-irrigation processes in the sediments. Thus, the incubation-derived sedimentary DO consumption rate was applied to analyze the correlation with the *in situ* nitrogen removal rate.

2.4. Sediment slurry incubation for potential rate determination

Potential rates of denitrification and anammox in the surface sediments were measured *via* slurry incubations, a simplified version of the technique devised by Thamdrup and Dalsgaard (2002). In brief, the slurry was prepared by mixing the surface sediments with the filtered (0.2 μm) bottom water in a 1:1 (v/v) ratio, and then homogenized and purged by helium gas for ~1 h to ensure an anoxic condition for the slurry tube (500 mL). Subsequently, 3 mL of premixed anoxic slurry was transferred into 12 mL gas-tight vials (Exetainers, Labco); the headspace of each vial was then purged with helium for approximately 1 min. In total, 15 vials for each sampling site were prepared, and all of the samples were pre-incubated for more than 24 h to completely eliminate the residual oxygen and background concentration of NO_x^-. After the pre-incubation, ^{15}N-labeled substrates ($^{15}NH_4Cl$ and $Na^{15}NO_3$) were injected into the vials and the slurries were again thoroughly mixed. Incubations were performed in the dark at room temperature (25 °C).

Three sets of tracer addition experiments (5 vials for each set) were designed. For sets A and B, $^{15}NO_3^-$ (Sigma-Aldrich, 98 ^{15}N at%) or $^{15}NH_4^+$ (Sigma-Aldrich, 98 ^{15}N at%) were added to the slurries, and the final concentrations were 100 μmol ^{15}N L^{-1}, respectively. For set C, both $^{15}NH_4^+$ and $^{14}NO_3^-$ were added and the final concentrations of both were 100 μmol L^{-1}.

For each set of slurry incubations, one of the five vials was fixed immediately after the ^{15}N tracer addition and assigned as initial (time of zero). All of the remaining vials were then fixed together after 2 h incubations. To terminate the incubation, 100 μL of saturated $HgCl_2$ solution was added to the vials to kill microbes. All of the fixed samples were kept upside down at room temperature (25 °C) in the dark before isotopic measurement. The rates were calculated from the incremental amount of the ^{15}N-labled product over the incubation time.

2.5. Sediment intact core incubation for in situ rate measurement

To obtain denitrification and anammox rates in undisturbed surface sediments, core incubations according to Trimmer et al. (2006) were used. Note that the intact core incubation was not applied to P3 due to logistical reasons. The intact sediment cores were equilibrated with oxygen-saturated bottom water in a tank overnight to rebuild sediment profiles after core collection. At each sampling site, fourteen intact cores in total were applied to perform the $^{15}NO_3^-$ concentration series experiment. Before the tracer addition, we measured the overlying water DO concentration in each intact core, and then the $^{15}NO_3^-$ (Sigma-Aldrich, 98 ^{15}N at%) was added into the overlying water to final concentrations of 20, 40, 60, 80, 120, 140, and 160 μmol L^{-1}. Each concentration occupied two intact cores as duplicate. All cores were sealed, with overlying water stirred by using a small stir bar (4 cm length) below the surface of the overlying water, driven by a large external magnet inside the incubation tank following the design of Trimmer et al. (2006). About 30 min of pre-incubation time were adopted to ensure a constant ratio between $^{14}NO_3^-$ and $^{15}NO_3^-$ in the denitrification zone (Hsu and Kao, 2013). Immediately following pre-incubation, one core of each concentration treatment was sacrificed and taken as initial, while the remaining cores were stopped after ~2 h incubation at *in situ* temperature (21–23 °C). To stop the incubation, we measured the DO concentration again and subsampled the sediment cores by mixing the overlying

water and the top 2 cm of sediments gently with a glass rod (Dalsgaard et al., 2000). A total of 3 mL of mixed slurry was sampled into a 12 mL gas-tight vial (Exetainer, Labco) containing 100 μL saturated $HgCl_2$ solution and a glass bead. Five replicates were sampled for each intact core. All of the vials were capped, and the headspace was quickly flushed with helium for approximately 1 min to replace the redundant air. Lastly, the samples were kept upside down at room temperature for later analysis. The difference of DO concentration in each core was applied to calculate the sedimentary DO consumption rate.

2.6. Chemical analysis

The concentration of NO_x^- was analyzed by vanadium (III) reduction with chemiluminescence detection (Braman and Hendrix, 1989). Sediment porosity was measured from the weight loss of a known amount of wet sediment after drying at 60 °C to a constant value. The dry sediment was acidified with 1 N HCl to remove inorganic carbon for 16 h, then organic carbon (OC) and organic nitrogen (ON) contents in the sediments were determined with a Carlo-Erba EA 2100 elemental analyzer (Kao et al., 2008). The ^{15}N labeled products in fixed samples, including the $^{29}N_2$, $^{30}N_2$, $^{45}N_2O$, and $^{46}N_2O$, were quantified using a Thermo Finnigan Delta^{plus} Advantage isotope ratio mass spectrometer, equipped with a Gas-Bench II and a PoraPlot Q GC column (Hsu and Kao, 2013).

2.7. Nitrogen removal rates calculation and uncertainty analysis

For the slurry incubation, the potential rates of denitrification and anammox were quantified using the $^{29}N_2$ and $^{30}N_2$ production rates, since no N_2O was detectable. We applied the quantification technique of Thamdrup and Dalsgaard (2002) for calculation. In set A, $^{28}N_2$, $^{29}N_2$ were assumed to be the products from both denitrification and anammox, while $^{30}N_2$ was solely sourced from denitrification. As only insignificant anammox rates were observed in sets B and C, the following equations were adapted to calculate the potential denitrification rate.

$$D_{potential} = P_{30} \times \left(\frac{1}{1 + r_{14-N_2}}\right)^{-2}, \tag{5}$$

$$r_{14-N_2} = D_{29}/2 \times D_{30}, \tag{6}$$

where $D_{potential}$ is the potential denitrification rate. P_{30} represents the production rate of $^{30}N_2$. r_{14}-N_2 is the ratio between $^{14}NO_3^-$ and $^{15}NO_3^-$ undergoing nitrate reduction, derived from N_2 production under the assumption that denitrification produces $^{28}N_2$, $^{29}N_2$ and $^{30}N_2$ through random isotope pairing (Hsu and Kao, 2013). The assumption of ignorable anammox throughout the study area was justified later.

In set C, $^{29}N_2$ was only produced from anammox in anaerobic sediments, thus the potential anammox rate was,

$$A_{potential} = P_{29} \times F_A, \tag{7}$$

where $A_{potential}$ denotes the potential anammox rate. P_{29} and F_A represent the production rate of $^{29}N_2$ and the labeling fraction of $^{15}NH_4^+$ in each experimental set, respectively.

For intact core incubations, the *in situ* denitrification and anammox rates were quantified based on the $^{29}N_2$, $^{30}N_2$, $^{45}N_2O$ and $^{46}N_2O$ production rates. To avoid the effect of $^{29}N_2$ that was produced from anammox on the r_{14}, we applied the r_{14}-N_2O ratio instead of r_{14}-N_2 to calculate the denitrification and anammox rates. For the purposes of this technique, denitrification was assumed to be the only quantitatively significant source of $^{45}N_2O$ and $^{46}N_2O$ during the intact core incubations (Trimmer et al., 2006). The total denitrification and anammox rates were derived from the sum of N_2 and N_2O production rates, using the following equations (Hsu and Kao, 2013),

$$D_{14} = 2(r_{14-N_2O} + 1) \times r_{14-N_2O} \times P_{30} + r_{14-N_2O} \times (2P_{46} + P_{45}), \tag{8}$$

$$r_{14-N_2O} = P_{45}/2 \times P_{46}, \tag{9}$$

$$A_{14} = 2 \times r_{14-N_2O} \times (P_{29} - 2 \times r_{14-N_2O} \times P_{30}), \tag{10}$$

where D_{14} and A_{14} represent the *in situ* denitrification and anammox rates, respectively, supported by the $^{14}NO_3^-$ in the environment. P_{45} and P_{46} denote the production rates of $^{45}N_2O$ and $^{46}N_2O$, respectively. Finally, the genuine nitrogen removal rates (P_{14}) were calculated by summing D_{14} and A_{14}.

$$P_{14} = D_{14} + A_{14} = 2r_{14-N_2O} \times [P_{29} + (1 - r_{14-N_2O}) \times P_{30}] + r_{14-N_2O} \times (2P_{46} + P_{45}). \tag{11}$$

To separate the sources of nitrate to fuel nitrogen removal in sediments, we applied the following equations to calculate the genuine nitrogen removal rate supported by the water-column-delivered nitrate ($P_{14}w$) and by the sedimentary coupled nitrification-denitrification ($P_{14}n$) (Hsu and Kao, 2013):

$$P_{14}w = P_{14} \times \frac{r_{14}w}{r_{14-N_2O}}, \tag{12}$$

$$P_{14}n = P_{14} - P_{14}w, \tag{13}$$

where $r_{14}w$ is the ratio of $^{14}NO_3^-$ to $^{15}NO_3^-$ concentration in the water column.

Using error propagation, we conducted the uncertainty analysis of the calculated fluxes in the following context based on Eqs. (14) and (15).

$$F = f(x_1, x_2, x_3), \tag{14}$$

$$\delta\_F = \sqrt{\left(\frac{\partial f}{\partial x_1}\right)^2 \times \delta\_x_1{}^2 + \left(\frac{\partial f}{\partial x_2}\right)^2 \times \delta\_x_2{}^2 + \left(\frac{\partial f}{\partial x_3}\right)^2 \times \delta\_x_3{}^2}, \tag{15}$$

where F is the flux of sedimentary nitrogen removal and N_2O production. x_1, x_2 and x_3 represent different error sources and δ_x_1, δ_x_2, and δ_x_3 denote the uncertainty of each error source. δ_F is the uncertainty of the calculated flux.

2.8. Statistical analysis

Pearson correlation analysis was applied to examine the correlations between nitrogen removal rates and environmental variables. A one-way analysis of variance (ANOVA) was performed to examine the spatial difference in relative magnitude of denitrification and anammox

Table 1
Environmental characteristics of the sampling sites in the Pearl River Estuary.

Sites	Depth (m)	T_b (°C)	S_b	$[NO_x^-]_b$ (μmol L^{-1})	$[OC]_s$ (mg C g^{-1})	$[ON]_s$ (mg N g^{-1})	C/N_s	Porosity	OPD (mm)
P3	9	20.9	0.2	190.3	11.77	0.77	15.35	0.66	0.8
A1	20	21.5	19.5	113.0	11.96	1.05	11.44	0.65	2.4
A3	7	21.2	21.6	90.4	2.79	0.16	17.15	0.59	4.0
A4	8	22.3	13.9	138.5	2.38	0.12	19.72	0.69	6.0
A6	9	23.1	26.6	55.0	3.39	0.24	14.21	0.57	2.0
A9	26	22.7	31.9	22.2	3.91	0.29	13.26	0.71	2.2

T_b and S_b denote temperature and salinity in the bottom water. Subscripts "b" and "s" represent bottom water and surface sediments, respectively. OPD is the oxygen penetration depth.

rates. All statistical analyses were conducted by using Statistical Package of Social Sciences (SPSS, version-19.0) at a 0.05 significance level.

3. Results

3.1. Environmental setting

The water depth of the sampling sites ranged from 7 to 26 m (Table 1). The bottom water temperature varied in a narrow range of 20.9–23.1 °C, while a distinct salinity gradient (0.2–31.9) was observed longitudinally. The concentrations of NO_x^- in bottom water ranged from 22.2 to 190.3 μmol L^{-1} and were significantly correlated to water salinity ($r = -0.995$, $p = 0.0004$), with higher concentration in low salinity water. The content of organic carbon and nitrogen in the surface sediments ranged from 2.38 to 11.96 mg C g^{-1} and from 0.12 to 1.05 mg N g^{-1}, respectively, displaying a large variation with higher content in the upper estuary. The porosity of sediments varied between 0.59 and 0.71. The additional descriptions of pore water chemistry, such as the concentrations of dissolved inorganic carbon, NO_x^- and ammonium, were detailed in Cai et al. (2015).

3.2. Dissolved oxygen

The DO concentrations in bottom water remained high at the sampling sites and ranged from 84.1 to 262.5 μmol L^{-1} (Fig. 2a). The highest DO concentration occurred at A3, while the lowest concentration appeared at the most upstream station, P3.

Below the sediment water interface, the DO concentration decreased dramatically downward to zero (Fig. 2a) with different OPDs. The OPD in the sampling sites varied from 0.8 to 6.0 mm (Table 1). The shallowest oxygen penetration appeared at P3, corresponding to the lowest bottom water DO concentration, while the deepest depth appeared at A4, corresponding to the lowest OC and ON contents in surface sediments (Fig. 2a and Table 1).

The sedimentary DO consumption rates, based on the diffusion method, ranged from 4.1 to 9.3 mmol m^{-2} d^{-1}, with the highest DO consumption rate occurring at A9 and the lowest rate at A4 (Fig. 2b). However, the DO consumption rates derived from the incubation method (7.3–42.0 mmol m^{-2} d^{-1}) were 1–6 times greater than those from the diffusion method, with higher rates appearing at the upstream stations (Fig. 2b).

3.3. Presence of anammox in surface sediments

Anaerobic slurry incubations were performed to confirm the presence of anammox metabolism, designated as sets B (incubation with $^{15}NH_4^+$) and C (incubation with $^{15}NH_4^+$ and $^{14}NO_3^-$) for the PRE surface sediments. Theoretically, no $^{29}N_2$ would be produced in set B since nitrite for anammox was absent after pre-incubation. While remarkable $^{29}N_2$ production rate should be detected after $^{14}NO_3^-$ addition in set C if anammox was present. Experimental results showed that the $^{29}N_2$ production in set C (0.6–4.5 nmol N mL^{-1} h^{-1}) were two orders of magnitude higher than that in set B (0–0.1 nmol N mL^{-1} h^{-1}), thus confirming the presence of anammox in the PRE surface sediments.

3.4. Potential denitrification and anammox rates

Potential denitrification and anammox rates varied from 26.9 to 94.4 nmol N mL^{-1} h^{-1} and from 0.6 to 4.5 nmol N mL^{-1} h^{-1}, respectively (Fig. 3). The potential denitrification rates were two orders of magnitude greater than potential anammox rates in the PRE sediments. Significant spatial differences in the potential denitrification and anammox rates were observed among the sampling sites (one-way ANOVA, $n = 6$, $p = 0.0002$ for potential denitrification and one-way ANOVA, $n = 6$, $p < 0.0001$ for potential anammox). The highest denitrification potential was detected at the most upstream station, P3, whereas the lowest rate was at A3, in the middle estuary. For the anammox potential, the highest rate occurred at A6, in the middle-lower estuary while the lowest appeared at nearby A4.

For the two nitrogen removal pathways in slurry incubations, anammox contributed only 1.27–5.11% to the total nitrogen loss, indicating that denitrification dominated the nitrogen removal pathway in the PRE sediments. This result validated the appropriateness of the assumption for the potential denitrification rate calculation in set A.

3.5. In situ denitrification and anammox rates

The *in situ* denitrification rates presented a downstream decreasing pattern in the PRE sediments and varied by over one order of magnitude from 32.2 to 707.7 μmol N m^{-2} h^{-1}, with the highest rate at A1 and the lowest at A9 (Fig. 4a). The rate was significantly negatively correlated to bottom water salinity ($r = -0.892$, $p = 0.042$), positively correlated to bottom water NO_x^- concentration ($r = 0.928$, $p = 0.022$) and sedimentary DO consumption rate ($r = 0.881$, $p = 0.048$) (Table 2). The *in situ* anammox rates ranged from 0 to 2.5 μmol N m^{-2} h^{-1} and were

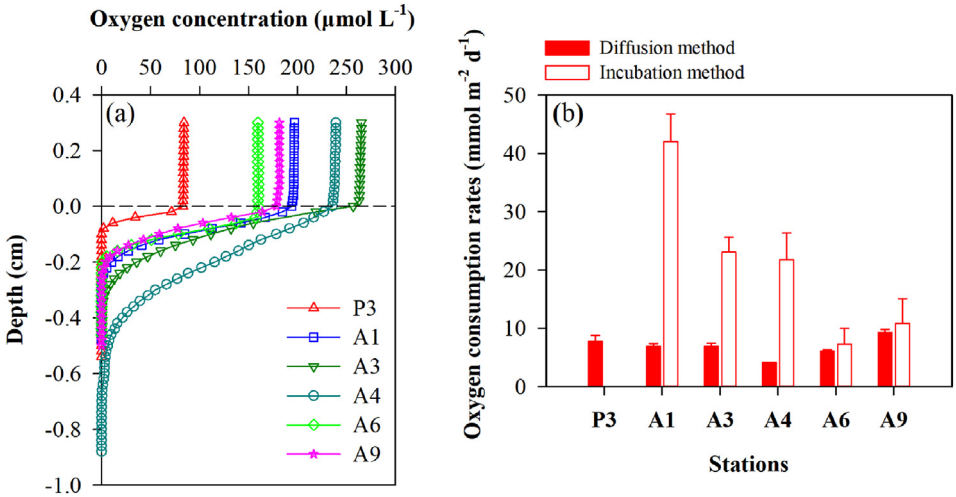

Fig. 2. The (a) profiles and (b) consumption rates of dissolved oxygen for the Pearl River Estuary sediments. The dashed line in (a) represents the sediment water interface. Vertical bars denote standard deviation.

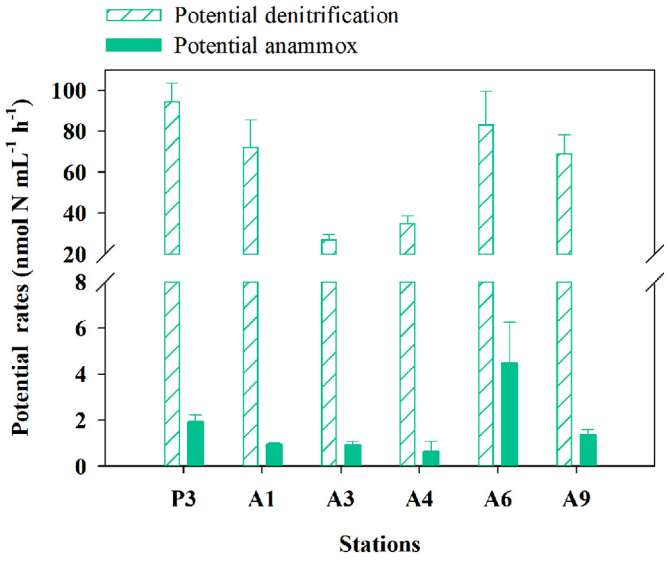

Fig. 3. The spatial distribution of potential rates for denitrification and anammox. Potential denitrification and anammox rates were calculated *via* experimental sets A and C, respectively. Vertical bars denote standard deviation of quadruplicate samples.

appreciably lower than the *in situ* denitrification rates, suggesting that anammox was a minor contributor (0–6.8%) to sedimentary nitrogen removal. Except for A3 and A4, where no anammox process was detected, the anammox rates were comparable across all sites, showing no downstream decreasing pattern (Fig. 4b). The only correlation observed for anammox against multiple environmental parameters was a negative relationship with respect to the corresponding C/N ($r = -0.946$, $p = 0.015$) and OPD ($r = -0.839$, $p = 0.076$) (Table 2). A higher proportional contribution of anammox to nitrogen removal was observed in the seaward sediments (Fig. 4b), where *in situ* denitrification became lower (Fig. 4a).

On the other hand, N_2O production was observed during the intact core incubation, ranging from 0.2 to 21.6 μmol N m^{-2} h^{-1}. The highest N_2O production rate occurred at A1, while the lowest appeared at A4 (Fig. 4d), differing from the seaward decreasing pattern for *in situ*

Table 2
Pearson correlation analysis between *in situ* nitrogen transformation rates and environmental factors in the Pearl River Estuary ($n = 5$). Only the coefficients are shown in the table. Bold numbers represent statistically significant correlations ($p < 0.05$).

Rates	Salinity	OC[a]	ON[a]	C/N	NO_x^-[b]	OPD	DO flux[c]
Denitrification	**−0.892**	0.449	0.423	0.263	**0.928**	0.583	**0.881**
Anammox	0.585	0.669	0.690	**−0.946**	−0.516	**−0.839**	−0.116
N_2	**−0.921**	0.386	0.359	0.334	**0.950**	0.647	0.841
N_2O	−0.228	**0.994**	**0.990**	−0.659	0.322	−0.336	0.848
$P_{14}w$	−0.675	0.798	0.783	−0.192	0.741	0.187	**0.923**
$P_{14}n$	**−0.897**	0.189	0.160	0.488	0.911	0.731	0.740

[a] The content in surface sediments.
[b] The concentrations in bottom water. OPD is the oxygen penetration depth.
[c] The incubation-derived DO consumption rate.

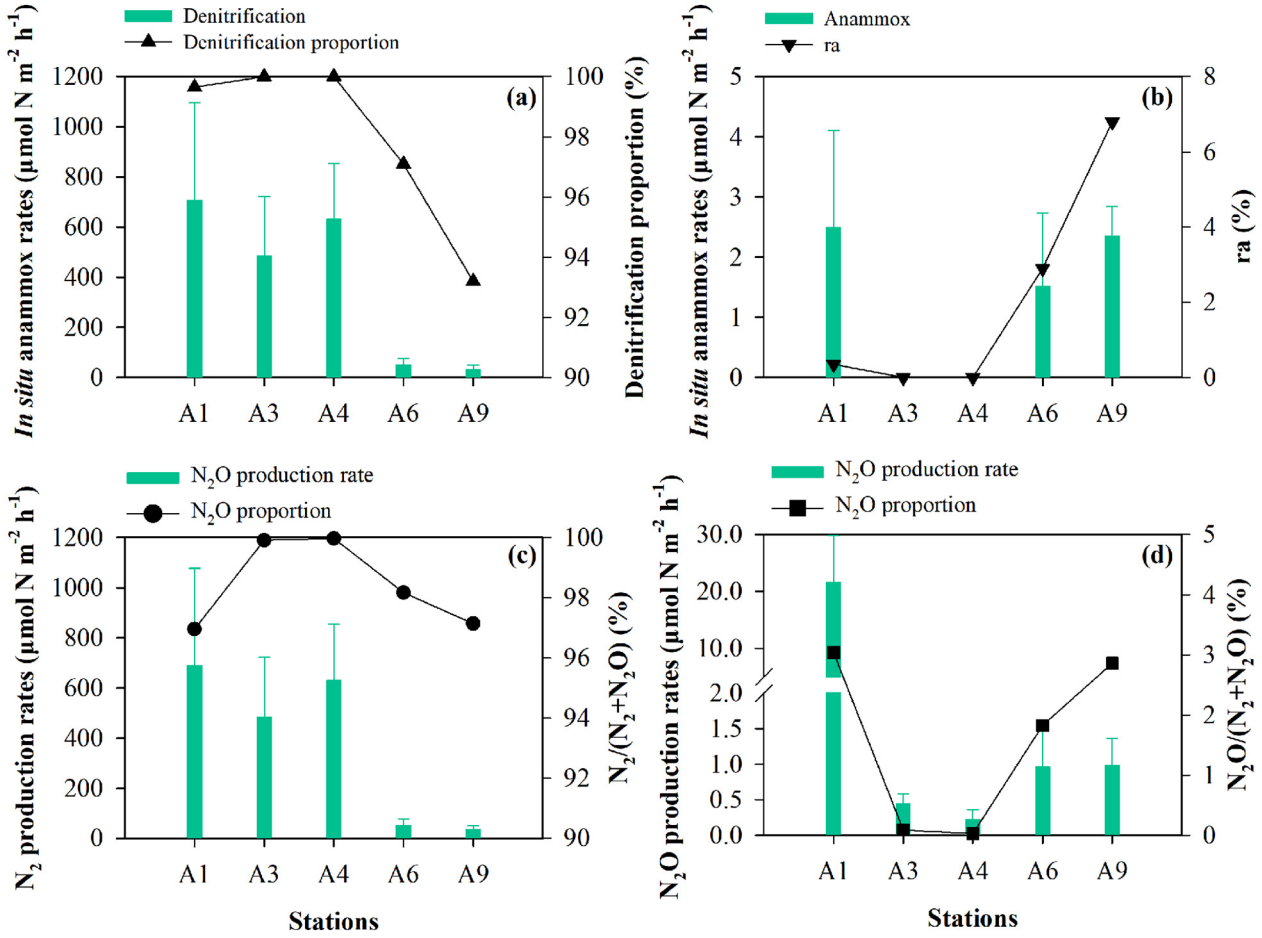

Fig. 4. The spatial distribution of *in situ* rates for (a) denitrification and the relative contribution of denitrification to total nitrogen removal, (b) anammox and the relative contribution of anammox to total nitrogen removal, (c) N_2 production rates and the proportional contribution of N_2 to total nitrogen loss, and (d) N_2O production rates and the proportional contribution of N_2O to total nitrogen loss in intact core incubations. Vertical bars denote standard deviation.

denitrification. In contrast, the total N_2 production rates were much higher, varying from 33.6 to 688.6 μmol N m^{-2} h^{-1} (Fig. 4c). The contributions of N_2O to total nitrogen loss ranged from 0.03 to 3.04% among the five sites, with a lower contribution in the middle estuary (Fig. 4d). Up to 3% of removed nitrogen was transformed to N_2O, indicating that the PRE sediment might play an important role in N_2O emission. Of the detected environmental factors, N_2O production rate correlated significantly with the contents of organic carbon ($r = 0.994$, $p = 0.001$) and nitrogen ($r = 0.990$, $p = 0.001$) in surface sediments (Table 2).

The nitrogen removal rates supported by sedimentary coupled nitrification-denitrification ($P_{14}n$) ranged from 31.1 to 466.8 μmol N m^{-2} h^{-1} (Fig. 5), and their contribution to total nitrogen removal was estimated to be as high as 56–90% (average of 76%). Obviously, nitrification in the aerobic sediments was the major source of NO_x^- for nitrogen removal in PRE sediments. Additionally, nitrogen removal supported by water-column-delivered NO_x^- ($P_{14}w$, *via* physical diffusion) contributed 10–44% (average of 24%) to total nitrogen loss with rates of 3.5–308.8 μmol N m^{-2} h^{-1} (Fig. 5), suggesting that physical diffusion of NO_x^- from the water column was significant but less important for nitrogen removal in the PRE sediments.

Among environmental parameters, $P_{14}n$ was negatively correlated to salinity ($r = -0.897$, $p = 0.039$) and positively correlated to sedimentary DO consumption rate ($r = 0.740$, $p = 0.153$) (Table 2), while $P_{14}w$ was positively correlated to the sedimentary organic carbon content ($r = 0.798$, $p = 0.105$), sedimentary organic nitrogen content ($r = 0.783$, $p = 0.117$), and the bottom water NO_x^- concentration ($r = 0.741$, $p = 0.152$) (Table 2).

4. Discussion

4.1. Nitrogen removal and environmental regulators

In the PRE sediments, denitrification was dominant, although rates varied among the different sites (Figs. 3 and 4a). The highly variable denitrification in space appeared to be driven by different environmental factors. The potentially effective environmental factors include bottom water NO_x^- concentration, bottom water salinity and sedimentary DO consumption rate. As stated previously, NO_x^- transported to sediments by diffusion was another important source for sedimentary nitrogen removal, accounting for 10–44% (Fig. 5). A positive correlation was observed between $P_{14}w$ and NO_x^- concentration (Table 2), which in turn

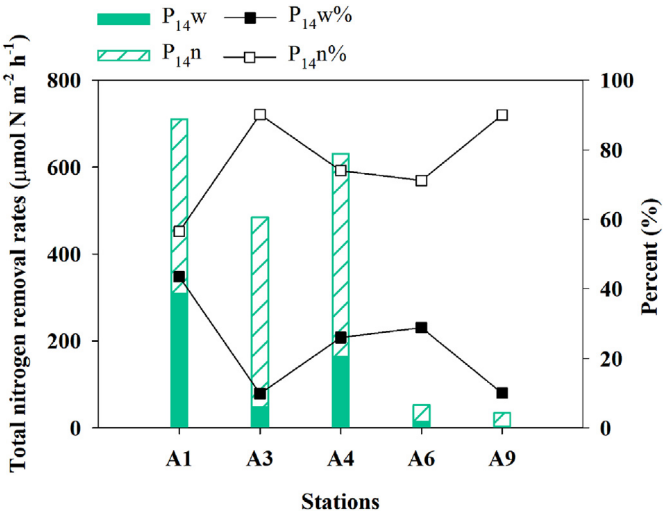

Fig. 5. The spatial distribution of the total nitrogen removal rates, supported by physical diffusion ($P_{14}w$) and coupled nitrification-denitrification ($P_{14}n$), and the proportional contribution of individual processes to the total nitrogen removal rate.

demonstrated the importance of NO_x^- diffusion in the regulation of sedimentary denitrification.

In addition to the effect of bottom water NO_x^- concentration, *in situ* denitrification rates were observed to be negatively correlated with bottom water salinity, indicating that salinity was another important regulator for sedimentary denitrification (Table 2). A significant inverse relationship of sedimentary denitrification rate and bottom water salinities was also observed in the Parker River Estuary and Rander Fjord Estuary (Giblin et al., 2010; Rysgaard et al., 1999). Moreover, in the Louisiana estuary, Seo et al. (2008) found that the sedimentary denitrification rate at the upstream sites was ~300% higher than that observed in the most downstream station, with the highest salinity. Rysgaard et al. (1999) proposed a mechanism by which salinity may diminish denitrification rates by cutting down the supply of nitrate from salinity-sensitive nitrification. Many previous studies indeed found that the nitrification rates decreased significantly as salinity increased in estuaries (Bernhard et al., 2005; Mondrup, 1999), indicating that salinity may inhibit nitrification in overlying water or sediments. Since in this study, sedimentary nitrification was the major process for fueling substrates for sedimentary nitrogen removal (Fig. 5), it could be inferred that high salinity constrains the nitrification and subsequently, the sedimentary denitrification rate.

In addition, oxygen in porewater may stimulate denitrification indirectly by enhancing sedimentary nitrification (Rysgaard et al., 1994), although denitrifiers undergo anaerobic metabolism. In our study, the *in situ* denitrification rate was positively correlated to the sedimentary DO consumption rate (Table 2), supporting the findings of Rysgaard et al. (1994). Indeed, the contribution of internal coupled nitrification-denitrification in sediments to total nitrogen loss ranged from 56% to 90% (Fig. 5). Previous studies also reported that coupled nitrification-denitrification played significant roles in nitrogen removal in various ecosystems, such as subtidal permeable sediments (Marchant et al., 2016), riverine suspended particles (Xia et al., 2016), and constructed wetland sediments (Tan et al., 2017).

Many studies have shown that organic matter is a significant factor regulating denitrification in sediments (Brin et al., 2014; Plummer et al., 2015). However, no significant correlations were observed between denitrification rates and the quantity or quality of sedimentary organic matter in our study (Table 2), indicating that organic matter was not a control factor for denitrification in PRE sediments. Moreover, temperature showed no correlation with the nitrogen removal rates ($r = -0.761$, $p = 0.135$ for denitrification and $r = 0.271$, $p = 0.659$ for anammox) in our study. Qian et al. (2018) reported that the PRE water body has distinct seasonal variations, rising from ~15 °C in the winter to ~30 °C in the summer. Such fluctuant temperature might play a critical role on the rates of nitrogen removal and associated N_2O production on a seasonal scale. As temperature showed little variation site to site (Table 1), its effects were not obvious in this study.

Relative to denitrification, anammox was a minor contributor to total sedimentary nitrogen removal at all the locations sampled (Fig. 4a and b). At A3 and A4, the anammox rate was not detectable *via* intact sediment core incubation, although anammox activity was observed in the anaerobic slurry incubation of the corresponding surface sediments (Fig. 3). The low content and quality of organics (high sedimentary C/N) and deep OPD might be responsible for the spatial variation of anammox rates in intact core incubations. Anammox rates were negatively correlated to the sedimentary C/N (Table 2), and it was speculated that the most important driver could be the high sedimentary C/N, since the partitioning of nitrogen loss between denitrification and anammox has been reported to be directly dependent on the C/N of the organic matter supply (Babbin et al., 2014; Babbin and Ward, 2013). Similarly, the anammox rate was negatively correlated to the OPD (Table 2). Since the OPD in sites A3 and A4 was the deepest (Fig. 2), it could therefore be inferred that the absence of anammox was caused by the inhibition of oxygen. Strous et al. (1997) also

Table 3
A comparison of sedimentary nitrogen removal rates at various regions. n.d. means not determined. Note that nitrogen removal rates in all listed studies were determined by using intact core incubation and isotope pairing technique.

Regions	Denitrification (μmol N m^{-2} h^{-1})	Anammox (μmol N m^{-2} h^{-1})	References
Constructed wetland, Australia	651.5–965.9	66.1–199.4	(Erler et al., 2008)
Apalachicola Bay, Mexico	1.4–12.3	0.4–1.1	(Gihring et al., 2010)
Jinpu Bay, China	0.1–13.7	0–1.5	(Yin et al., 2014)
Coastal Greenland	1.5–10.4	0.1–3.8	(Rysgaard et al., 2004)
Arctic Shelf	3.6–16.1	0.1–0.3	(McTigue et al., 2016)
Danshuei River, Taiwan	125.7	13.0	(Hsu and Kao, 2013)
Tama River Estuary, Japan	214–1260	n.d.	(Usui et al., 2001)
Thames Estuary, England	6.1–192.9	6.6–48.9	(Trimmer et al., 2006)
St. Lawrence Estuary, Canada	11.3	5.5	(Crowe et al., 2012)
Pearl River Estuary, China	32.2–707.7	0–2.5	This study

indicated that the anammox process appears only under strict anaerobic conditions, according to their experimental results, in which anammox activity was reversibly inhibited when the oxygen level increased to 1 μmol L^{-1}. However, the C/N and OPD were synergistic, and the anammox activities in natural sediments were thus co-affected by those two variables.

4.2. Hotspot of nitrogen loss and the role of particulate organic matter

If we compared our results with other estimations at various regions globally, the nitrogen removal rates we estimated in the PRE sediments were higher than most of the other regions, including continental shelf and estuarine sediments (Table 3). However, our sedimentary denitrification rates were comparable to those reported in constructed wetlands (Erler et al., 2008) and Tama River Estuary (Usui et al., 2001). We thus concluded that the PRE sediments acted as an important hotspot for nitrogen removal.

We found that nitrogen was removed *via* N_2 and N_2O release, with N_2 as the dominant product in the PRE sediments (Fig. 4c and d). To quantify the sedimentary nitrogen removal flux, we zoned the study area into five rectangles, with an area of 105, 179, 211, 383, and 302 km^2, respectively, as indicated in Cai et al. (2015). Total nitrogen removal flux was estimated by integrating the site-specific fluxes over the study area. We derived a nitrogen removal flux of $8.1 \pm 2.0 \times 10^6$ mol N d^{-1}, implying that the PRE sediments were significant nitrogen removal hotspots. Our finding was ~4 times lower than the estimate in Cai et al. (2015) during the same cruise, which demonstrated a benthic nitrogen removal flux of $3.6 \pm 0.3 \times 10^7$ mol N d^{-1} based on the $^{224}Ra/^{228}Th$ disequilibrium approach. Cai et al. (2015) demonstrated that the dominant nitrogen removal pathway in sediments was derived from non-local transport or bio-irrigation. However, only the nitrogen removal that was fueled by organic matter remineralization and physical diffusive NO_x^- was constrained in this study. Bio-irrigation promotes the diffusion of DO and NO_x^- from overlying water to sediments by increasing the incurvate interface area and subsequently stimulates the sedimentary nitrification and denitrification. As mentioned above, both water column and sediment-produced NO_x^- sustained denitrification and anammox in the PRE sediments. Based on our study, the removal flux that was supported by sedimentary nitrification was $6.0 \pm 1.5 \times 10^6$ mol N d^{-1}, suggesting that nitrogen was mainly removed *via* allochthonous or autochthonous particulate organic matter in sediments. The riverine input fluxes of NH_4^+ and particulate organic nitrogen (PON) were approximately 8.5×10^6 mol N d^{-1} and 1.1×10^7 mol N d^{-1} (Cai et al., 2015; He et al., 2010), respectively. Since that PON undergoes ammonification before sedimentary nitrification, we assumed that all the riverine inputted NH_4^+ was converted to PON, and ~31% of the total PON (allochthonous and autochthonous) input (~2.0×10^7 mol N d^{-1}) was thus removed *via* sedimentary nitrification-denitrification. This estimate likely to be on the conservative side, and the actual PON removal *via* sedimentary nitrification-denitrification plays a greater role than suggested above. Another removal flux of $2.1 \pm 0.6 \times 10^6$ mol N d^{-1} in sediments was supported by the water-column-delivered NO_x^-, accounting for ~8% of the riverine input if the riverine flux was 2.5×10^7 mol N d^{-1} for nitrate (Cai et al., 2015).

The total nitrogen input into the estuary is ~4.5×10^7 mol N d^{-1}, with 24.7% of it represented by PON. The total nitrogen removal is $8.1 \pm 2.0 \times 10^6$ mol N d^{-1}; ~74% of total nitrogen removal depends on PON linking nitrogen in the water column to sedimentary nitrogen pool. Generally, the PRE sediments performed as a significant filter of organic nitrogen; however, the major parts of riverine reactive nitrogen were still retained in the ecosystem.

4.3. Sedimentary N_2O emission

Much higher N_2 production than N_2O production rates indicated that N_2 was the dominant end-product of nitrogen removal (Fig. 4c and d). In addition to N_2 production, the sedimentary N_2O production yielded 0.03–3% of the total nitrogen loss, with rates of 0.2–21.6 μmol N m^{-2} h^{-1} during the intact core incubation (Fig. 4d). Similar intertidal sediment N_2O production rates were reported in other studies, such as 0.2–25.2 μmol N_2O m^{-2} h^{-1} in the Humber Estuary (Barnes and Owens, 1999) and 0.01–0.9 μmol N_2O m^{-2} h^{-1} in the Yellow River Estuary (Sun et al., 2014). The N_2O production rates in this study were positively correlated to the sedimentary OC and ON contents (Table 2), and the N_2O/N_2 was significantly correlated to the C/N ($r = -0.950$, $p = 0.013$), indicating that the quantity and quality of organic matter likely had significant impacts on the N_2O yield in the PRE sediments.

Similarly, we calculated the N_2O flux to be $7.3 \pm 2.1 \times 10^4$ mol N d^{-1} by multiplying production rate by sediment area. The relative high uncertainties in the fluxes of nitrogen removal and N_2O release were mainly caused by the spatial variations in nitrogen removal rates and N_2O production rate. A total N_2O flux of $2.1 \pm 1.1 \times 10^5$ mol N d^{-1} in the PRE was reported by Lin et al. (2016), in which spatiotemporal variation of N_2O in surface water had been documented. Dividing the N_2O emission flux that produced from sedimentary denitrification by the total N_2O emission flux, the sedimentary N_2O production would occupy ~35% of the daily N_2O emission, indicating that the PRE sediments might also acted as a N_2O source. However, nitrification or nitrate reduction in the water column was other significant N_2O contributors in the PRE. Further studies are still needed to elucidate the roles of nitrification and denitrification in the N_2O budget.

5. Conclusions

We examined the nitrogen removal pathways and quantified the *in situ* denitrification and anammox with associated gaseous nitrogen production rates in the PRE sediments by applying slurry and intact sediment core incubations. Sedimentary nitrogen removal was predominated by denitrification relative to a minimal contribution from

anammox. Among the detected environmental factors, salinity, bottom water NO_x^- (nitrate and nitrite) concentration, sedimentary organic matter and dissolved oxygen consumption rates were important denitrification and anammox rates regulators. We found that sedimentary nitrogen removal involved mainly particulate organic form (allochthonous or autochthonous) deposited onto sediments, rather than inorganic forms in overlying water. Meanwhile, the PRE sediments also acted as a N_2O source with a flux of $7.3 \pm 2.1 \times 10^4$ mol N d^{-1}, equivalent to ~35% of the daily N_2O emissions in the PRE.

Acknowledgement

This is State Key Laboratory of Marine Environment Science contribution NO. melpublication2018258. Special acknowledgment to intensive field and laboratory works by Lingfeng Liu and Li Tian. This study was supported by the National Natural Science Foundation of China (NSFC #41721005, #41561164019 and #2015CB954003). The work described in this paper was partially supported by a grant from the Research Grants Council of the Hong Kong Special Administrative Region, China (Project No. T21-602/16R). We are grateful to anonymous reviewers for their constructive comments.

References

Babbin, A.R., Ward, B.B., 2013. Controls on nitrogen loss processes in Chesapeake Bay sediments. Environ. Sci. Technol. 47 (9), 4189–4196. https://doi.org/10.1021/es304842r.

Babbin, A.R., Richard, G.K., Allan, H.D., Bess, B.W., 2014. Organic matter stoichiometry, flux, and oxygen control nitrogen loss in the ocean. Science 344, 406–408. https://doi.org/10.1126/science.1248364.

Barnes, J., Owens, N.J.P., 1999. Denitrification and nitrous oxide concentrations in the Humber Estuary, UK, and adjacent coastal zones. Mar. Pollut. Bull. 37 (3–7), 247–260. https://doi.org/10.1016/S0025-326X(99)00079-X.

Bernhard, A.E., Donn, T., Giblin, A.E., Stahl, D.A., 2005. Loss of diversity of ammonia-oxidizing bacteria correlates with increasing salinity in an estuary system. Environ. Microbiol. 7 (9), 1289–1297. https://doi.org/10.1111/j.1462-2920.2005.00808.x.

Braman, R.S., Hendrix, S.A., 1989. Nanogram nitrite and nitrate determination in environmental and biological materials by vanadium (III) reduction with chemiluminescence detection. Anal. Chem. 61 (24), 2715–2718.

Brin, L.D., Giblin, A.E., Rich, J.J., 2014. Environmental controls of anammox and denitrification in southern New England estuarine and shelf sediments. Limnol. Oceanogr. 59 (3), 851–860. https://doi.org/10.4319/lo.2014.59.3.0851.

Cai, P., Shi, X., Hong, Q., Li, Q., Liu, L., Guo, X., Dai, M., 2015. Using $^{224}Ra/^{228}Th$ disequilibrium to quantify benthic fluxes of dissolved inorganic carbon and nutrients into the Pearl River Estuary. Geochim. Cosmochim. Acta 170, 188–203. https://doi.org/10.1016/j.gca.2015.08.015.

Crowe, S.A., Canfield, D.E., Mucci, A., Sundby, B., Maranger, R., 2012. Anammox, denitrification and fixed-nitrogen removal in sediments from the Lower St. Lawrence Estuary. Biogeosciences 9 (11), 4309–4321. https://doi.org/10.5194/bg-9-4309-2012.

Dai, M., Guo, X., Zhai, W., Yuan, L., Wang, B., Wang, L., Cai, P., Tang, T., Cai, W.-J., 2006. Oxygen depletion in the upper reach of the Pearl River estuary during a winter drought. Mar. Chem. 102 (1–2), 159–169. https://doi.org/10.1016/j.marchem.2005.09.020.

Dalsgaard, T., Nielsen, L.P., Brotas, V., Viaroli, P., Underwood, G.J.C., Nedwell, D.B., Sundbäck, K., Rysgaard, S., Miles, A., Bartoli, M., Dong, L.F., Thornton, D.C.O., Ottosen, L.D.M., Castaldelli, G., Risgaard-Petersen, N., 2000. Protocol Handbook for NICE Nitrogen Cycling in Estuaries. National Environmental Research Institute, Copenhagen, Denmark.

Deegan, L.A., Johnson, D.S., Warren, R.S., Peterson, B.J., Fleeger, J.W., Fagherazzi, S., Wollheim, W.M., 2012. Coastal eutrophication as a driver of salt marsh loss. Nature 490 (7420), 388–392. https://doi.org/10.1038/nature11533.

Devol, A.H., 2015. Denitrification, anammox, and N_2 production in marine sediments. Annu. Rev. Mar. Sci. 7, 403–423. https://doi.org/10.1146/annurev-marine-010213-135040.

Dong, L.F., Sobey, M.N., Smith, C., Rusmana, I., Phillips, W., Stott, A., Osborn, A.M., Nedwell, D.B., 2011. Dissimilatory reduction of nitrate to ammonium (DNRA) not denitrification or anammox dominates benthic nitrate reduction in tropical estuaries. Limnol. Oceanogr. 56 (1), 279–291. https://doi.org/10.4319/lo.2011.56.1.0279.

Engström, P., Penton, C.R., Devol, A.H., 2009. Anaerobic ammonium oxidation in deep-sea sediments off the Washington margin. Limnol. Oceanogr. 54 (5), 1643–1652 (doi:Anaerobic ammonium oxidation in deep-sea sediments off the Washington margin).

Erler, D.V., Eyre, B.D., Davison, L., 2008. The contribution of anammox and denitrification to sediment N_2 production in a surface flow constructed wetland. Environ. Sci. Technol. 42 (24), 9144–9150. https://doi.org/10.1021/es801175t.

Fernandes, S.O., Michotey, V.D., Guasco, S., Bonin, P.C., Bharathi, P.A.L., 2012. Denitrification prevails over anammox in tropical mangrove sediments (Goa, India). Mar. Environ. Res. 74, 9–19. https://doi.org/10.1016/j.marenvres.2011.11.008.

Giblin, A.E., Weston, N.B., Banta, G.T., Tucker, J., Hopkinson, C.S., 2010. The effects of salinity on nitrogen losses from an oligohaline estuarine sediment. Estuar. Coasts 33 (5), 1054–1068. https://doi.org/10.1007/s12237-010-9280-7.

Gihring, T.M., Canion, A., Riggs, A., Huettel, M., Kostka, J.E., 2010. Denitrification in shallow, sublittoral Gulf of Mexico permeable sediments. Limnol. Oceanogr. 55 (1), 43–54. https://doi.org/10.4319/lo.2010.55.1.0043.

He, B., Dai, M., Huang, W., Liu, Q., Chen, H., Xu, L., 2010. Sources and accumulation of organic carbon in the Pearl River Estuary surface sediment as indicated by elemental, stable carbon isotopic, and carbohydrate compositions. Biogeosciences 7 (10), 3343–3362. https://doi.org/10.5194/bg-7-3343-2010.

Hsu, T.C., Kao, S.J., 2013. Technical note: simultaneous measurement of sedimentary N_2 and N_2O production and a modified ^{15}N isotope pairing technique. Biogeosciences 10 (12), 7847–7862. https://doi.org/10.5194/bg-10-7847-2013.

Huang, X.P., Huang, L.M., Yue, W.Z., 2003. The characteristics of nutrients and eutrophication in the Pearl River estuary, South China. Mar. Pollut. Bull. 47 (1–6), 30–36. https://doi.org/10.1016/S0025-326X(02)00474-5.

Kao, S.J., Liu, K.K., Hsu, S.C., Chang, Y.P., Dai, M.H., 2008. North Pacific-wide spreading of isotopically heavy nitrogen during the last deglaciation: evidence from the western Pacific. Biogeosciences 5 (6), 1641–1650. https://doi.org/10.5194/bg-5-1641-2008.

Lin, H., Dai, M., Kao, S.J., Wang, L., Roberts, E., Yang, J.Y.T., Huang, T., He, B., 2016. Spatio-temporal variability of nitrous oxide in a large eutrophic estuarine system: the Pearl River Estuary, China. Mar. Chem. 182, 14–24. https://doi.org/10.1016/j.marchem.2016.03.005.

Liu, J.P., Xue, Z., Ross, K., Yang, Z.S., Gao, S., 2009. Fate of sediments delivered to the sea by Asian large rivers: long-distance transport and formation of remote alongshore clinothems. Sediment. Rec. 7 (4), 4–9.

Mao, Q., Shi, P., Yin, K., Gan, J., Qi, Y., 2004. Tides and tidal currents in the Pearl River Estuary. Cont. Shelf Res. 24 (16), 1797–1808. https://doi.org/10.1016/j.csr.2004.06.008.

Marchant, H.K., Holtappels, M., Lavik, G., Ahmerkamp, S., Winter, C., Kuypers, M.M., 2016. Coupled nitrification–denitrification leads to extensive N loss in subtidal permeable sediments. Limnol. Oceanogr. https://doi.org/10.1002/lno.10271.

McTigue, N.D., Gardner, W.S., Dunton, K.H., Hardison, A.K., 2016. Biotic and abiotic controls on co-occurring nitrogen cycling processes in shallow Arctic shelf sediments. Nat. Commun. 7, 13145. https://doi.org/10.1038/ncomms13145.

Mondrup, T., 1999. Salinity effects on nitrogen dynamics in estuarine sediment investigated by a Plug-Flux method. Biol. Bull. 197 (2), 287–288. https://doi.org/10.2307/1542656.

Mulder, A., Graaf, A.A., Robertson, L.A., Kuenen, J.G., 1995. Anaerobic ammonium oxidation discovered in a denitrifying fluidized bed reactor. FEMS Microbiol. Ecol. 16, 177–184. https://doi.org/10.1111/j.1574-6941.1995.tb00281.x.

Nicholls, J.C., Trimmer, M., 2009. Widespread occurrence of the anammox reaction in estuarine sediments. Aquat. Microb. Ecol. 55 (2), 105–113. https://doi.org/10.3354/ame01285.

Nixon, S.W., Ammerman, J.W., Atkinson, L.P., Berounsky, V.M., Billen, G., Boicourt, W.C., Boynton, W.R., Church, T.M., Ditoro, D.M., Elmgren, R., 1996. The fate of nitrogen and phosphorus at the land sea margin of the North Atlantic Ocean. Biogeochemistry 35 (1), 141–180. https://doi.org/10.1007/BF02179826.

Pennino, M.J., Kaushal, S.S., Murthy, S.N., Blomquist, J.D., Cornwell, J.C., Harris, L.A., 2016. Sources and transformations of anthropogenic nitrogen along an urban river–estuarine continuum. Biogeosciences 13 (22), 6211–6228. https://doi.org/10.5194/bg-13-6211-2016.

Plummer, P., Tobias, C., Cady, D., 2015. Nitrogen reduction pathways in estuarine sediments: influences of organic carbon and sulfide. J. Geophys. Res. Biogeosci. 120 (9). https://doi.org/10.1002/2015JG003057.

Qian, W., Gan, J., Liu, J., He, B., Lu, Z., Guo, X., Wang, D., Guo, L., Huang, T., Dai, M., 2018. Current status of emerging hypoxia in a eutrophic estuary: the lower reach of the Pearl River Estuary, China. Estuar. Coast. Shelf Sci. 205, 58–67. https://doi.org/10.1016/j.ecss.2018.03.004.

Rockstrom, J., 2009. A safe operating space for humanity. Nature 461, 472–475. https://doi.org/10.1038/461472a.

Rysgaard, S., Risgaard-Petersen, N., Sloth, N.P., Jensen, K., Nielsen, L.P., 1994. Oxygen regulation of nitrification and denitrification in sediments. Limnol. Oceanogr. 39, 1643–1652. https://doi.org/10.4319/lo.1994.39.7.1643.

Rysgaard, S., Thastum, P., Dalsgaard, T., Christensen, P., Sloth, N., 1999. Effects of salinity on NH_4^+ adsorption capacity, nitrification, and denitrification in Danish estuarine sediments. Estuaries 22 (1), 21–30. https://doi.org/10.2307/1352923.

Rysgaard, S., Glud, R.N., Risgaard-Petersen, N., Dalsgaard, T., 2004. Denitrification and anammox activity in Arctic marine sediments. Limnol. Oceanogr. 49 (5). https://doi.org/10.4319/lo.2004.49.5.1493.

Schlesinger, W.H., 2009. On the fate of anthropogenic nitrogen. Proc. Natl. Acad. Sci. U. S. A. 106 (1), 203–208. https://doi.org/10.1073/pnas.0810193105.

Schulz, H.D., 1999. Quantification of early diagenesis: dissolved constituents in pore water and signals in the solid phase. In: Schulz, H.D., Zabel, Matthias (Eds.), Marine Geochemistry. Springer-Verlag, Berlin Heidelberg.

Seitzinger, S.P., 1988. Denitrification in freshwater and coastal marine ecosystems: ecological and geochemical significance. Limnol. Oceanogr. 33 (4part2), 702–724.

Seitzinger, S., Harrison, J.A., Böhlke, J.K., Bouwman, A.F., Lowrance, R., Peterson, B., Tobias, C., Van Drecht, G., 2006. Denitrification across landscapes and waterscapes: a synthesis. Ecol. Appl. 16 (6), 2064–2090. https://doi.org/10.1890/1051-0761(2006)016[2064:DALAWA]2.0.CO;2.

Seitzinger, S.P., Mayorga, E., Bouwman, A.F., Kroeze, C., Beusen, A.H.W., Billen, G., Van Drecht, G., Dumont, E., Fekete, B.M., Garnier, J., Harrison, J.A., 2010. Global river nutrient export: a scenario analysis of past and future trends. Glob. Biogeochem. Cycles 24 (4). https://doi.org/10.1029/2009gb003587 (n/a-n/a).

Seo, D.C., Yu, K., Delaune, R.D., 2008. Influence of salinity level on sediment denitrification in a Louisiana estuary receiving diverted Mississippi River water. Arch. Agron. Soil Sci. 54 (3), 249–257. https://doi.org/10.1080/03650340701679075.

Strous, M., Van Gerven, E., Kuenen, J.G., Jetten, M., 1997. Effects of aerobic and microaerobic conditions on anaerobic ammonium-oxidizing (anammox) sludge. Appl. Environ. Microbiol. 63 (6), 2446–2448.

Sun, Z., Wang, L., Mou, X., Jiang, H., Sun, W., 2014. Spatial and temporal variations of nitrous oxide flux between coastal marsh and the atmosphere in the Yellow River estuary of China. Environ. Sci. Pollut. Res. 21 (1), 419–433. https://doi.org/10.1007/s11356-013-1885-5.

Tan, E., Hsu, T.-C., Huang, X., Lin, H.-J., Kao, S.J., 2017. Nitrogen transformations and removal efficiency enhancement of a constructed wetland in subtropical Taiwan. Sci. Total Environ. 601–602, 1378–1388. https://doi.org/10.1016/j.scitotenv.2017.05.282.

Teixeira, C., Magalhaes, C., Joye, S.B., Bordalo, A.A., 2012. Potential rates and environmental controls of anaerobic ammonium oxidation in estuarine sediments. Aquat. Microb. Ecol. 66 (1), 23–32. https://doi.org/10.3354/ame01548.

Teixeira, C., Magalhães, C., Joye, S.B., Bordalo, A.A., 2016. Response of anaerobic ammonium oxidation to inorganic nitrogen fluctuations in temperate estuarine sediments. J. Geophys. Res. Biogeosci. https://doi.org/10.1002/2015JG003287.

Thamdrup, B., Dalsgaard, T., 2002. Production of N_2 through anaerobic ammonium oxidation coupled to nitrate reduction in marine sediments. Appl. Environ. Microbiol. 68 (3), 1312–1318. https://doi.org/10.1128/aem.68.3.1312-1318.2002.

Trimmer, M., Nicholls, J.C., 2009. Production of nitrogen gas via anammox and denitrification in intact sediment cores along a continental shelf to slope transect in the North Atlantic. Limnol. Oceanogr. 54, 577–589. https://doi.org/10.4319/lo.2009.54.2.0577.

Trimmer, M., Risgaard-Petersen, N., Nicholls, J.C., Engström, P., 2006. Direct measurement of anaerobic ammonium oxidation (anammox) and denitrification in intact sediment cores. Mar. Ecol. Prog. Ser. 326, 37–47. https://doi.org/10.3354/meps326037.

Usui, T., Koike, I., Ogura, N., 2001. N_2O production, nitrification and denitrification in an estuarine sediment. Estuar. Coast. Shelf Sci. 52 (6), 769–781. https://doi.org/10.1006/ecss.2000.0765.

Xia, X., Jia, Z., Liu, T., Zhang, S., Zhang, L., 2016. Coupled nitrification-denitrification caused by suspended sediment (SPS) in rivers: importance of SPS size and composition. Environ. Sci. Technol. https://doi.org/10.1021/acs.est.6b03886.

Yin, G., Hou, L., Zong, H., Ding, P., Liu, M., Zhang, S., Cheng, X., Zhou, J., 2014. Denitrification and anaerobic ammonium oxidization across the sediment–water interface in the hypereutrophic ecosystem, Jinpu Bay, in the northeastern coast of China. Estuar. Coasts 38 (1), 211–219. https://doi.org/10.1007/s12237-014-9798-1.

Zhang, S., Lu, X.X., Higgitt, D.L., Chen, C.T.A., Han, J., Sun, H., 2008. Recent changes of water discharge and sediment load in the Zhujiang (Pearl River) Basin, China. Glob. Planet. Chang. 60 (3–4), 365–380. https://doi.org/10.1016/j.gloplacha.2007.04.003.

Zhang, W., Zheng, J., Xiaomei, J., Hoitink, A.J.F., van der Vegt, M., Zhu, Y., 2013. Surficial sediment distribution and the associated net sediment transport pattern in the Pearl River Estuary, South China. Cont. Shelf Res. 61–62, 41–51. https://doi.org/10.1016/j.csr.2013.04.011.